Deep Learning-based Range-Doppler Map Reconstruction for 1-bit Quantized PMCW Systems

Hyunjoung Lee, Seonmin Cho, and Seongwook Lee
Department of Electrical and Electronics Engineering
College of ICT Engineering, Chung-Ang University
Seoul, Republic of Korea
{jku2840, tjsals4514, seongwooklee}@cau.ac.kr

***Abstract*—Reliable target detection in phase-modulated continuous-wave (PMCW) radar systems relies on the formation of high-resolution range-Doppler (RD) maps. However, the use of 1-bit analog-to-digital converters (ADCs) for high-rate sampling in PMCW radar systems retains only the sign information of the received signal, resulting in a loss of amplitude information. This quantization process introduces severe noise across the entire RD map, thereby degrading target detection performance. In this paper, we propose a U-Net-based deep learning network to reconstruct high-quality RD maps from noise-distorted RD maps obtained using 1-bit ADCs in PMCW radar systems. The network is trained using paired datasets consisting of noise-distorted RD maps and corresponding refined RD maps, where the refined maps are generated using a kurtosis-based filtering algorithm. The proposed method effectively mitigates nonlinear distortions that cannot be corrected by conventional fast Fourier transform (FFT) and windowing-based processing. Specifically, the proposed method achieves a peak sidelobe level (PSL) of -46.19 dB and a signal-to-interference-plus-noise ratio (SINR) of -23.14 dB, improving PSL by 31.5 dB and SINR by 13.2 dB over conventional 1-bit FFT processing. In addition, it outperforms the multi-bit ADC-based FFT processing by 18.35 dB in PSL. These results demonstrate that the proposed method effectively enhances target detection performance in PMCW radar systems using 1-bit ADCs.**

***Index Terms*—1-bit analog-to-digital converter (ADC), deep neural networks, phase-modulated continuous-wave (PMCW) radar systems, quantization artifact suppression.**

I. Introduction

Integrated sensing and communication (ISAC) has been widely recognized as a key enabler for sixth-generation wireless networks [1]. Among various candidate waveforms for ISAC systems, phase-modulated continuous-wave (PMCW) radar has attracted significant attention [2]. Compared to conventional frequency-modulated continuous-wave radar, PMCW offers flexible code design, strong robustness against mutual interference, and seamless compatibility with multiple-input multiple-output configurations [3]. Specifically, the adoption of well-designed pseudorandom binary sequences (PRBSs) allows PMCW systems to achieve a sharp mainlobe and significantly low sidelobes levels in the range domain [4]. In addition, code-domain processing inherent to PMCW naturally supports multi-user operation and efficient coexistence with communication signals. These properties make PMCW particularly attractive for autonomous driving radar platforms, where scalability and reliable operation in interference limited environments are essential.

Despite these advantages, practical deployment of PMCW radar faces stringent hardware constraints. PMCW transmits digitally modulated sequences whose chip rate equals the waveform bandwidth. The receiver must therefore sample the incoming signal at rates ranging from several hundred MS/s to multiple GS/s. Such high sampling rates significantly increase power consumption and system cost, which makes multi-bit analog-to-digital converter (ADC) difficult to integrate into embedded automotive platforms. These constraints have motivated the use of 1-bit ADC for hardware simplification. However, 1-bit quantization discards amplitude information and introduces nonlinear distortions, which result in elevated sidelobes and structural artifacts in the range-Doppler (RD) domain. Crucially, the loss of amplitude information hinders the sharpening of correlation peaks in the RD domain, making it difficult to distinguish target mainlobes from elevated quantization-induced sidelobes. Consequently, the presence of strong scattering objects degrades the detectability of low radar cross section (RCS) targets and the effective dynamic range.

Existing studies have explored various strategies to mitigate the performance degradation caused by 1-bit quantization. For example, joint optimization of transmission codes and reception filters has been proposed to enhance autocorrelation properties, while classical windowing is applied to the received signal prior to fast Fourier transform (FFT) operations to mitigate spectral leakage [5], [6]. Recently, learning-based methods have also been investigated to enhance RD maps directly from quantized measurements [7]. Specifically, joint transmit-receive optimization ensures a refined correlation response with minimized sidelobe levels prior to the quantization process. However, nonlinear artifacts such as sidelobe regrowth and noise floor elevation persist after quantization and cannot be suppressed by design-based or linear processing methods alone. Although learning-based approaches are in principle capable of addressing nonlinear distortions, many existing networks are trained using simplified supervisory signals that fail to capture the distortion characteristics of 1-bit quantized RD maps. As a result, these methods show limited capability in handling nonlinear artifact patterns observed under practical operating conditions. These limitations become more pronounced in high dynamic range or multi-

target scenarios.

In this paper, we propose a learning-based restoration method that recovers high-quality RD maps from single 1-bit PMCW measurements. A key observation is that kurtosis-refined RD maps provide structurally faithful supervision for the network. By exploiting the highly non-Gaussian and impulsive nature of 1-bit quantization artifacts, kurtosis serves as a robust statistical metric to distinguish nonlinear distortions from legitimate target returns. The U-Net is trained using these refined maps as the ground truth, enabling the network to effectively suppress Doppler sidelobe regrowth and noise floor elevation while preserving target peak morphology. The proposed method operates directly on distorted 1-bit RD maps without requiring additional hardware complexity and generalizes across varying ranges, Doppler values, transmit sequences, and multi-target scenarios. These capabilities enable practical deployment of 1-bit PMCW radar by providing reliable RD restoration while retaining its power and cost advantages for automotive systems.

II. Radar Signal Processing of SISO-PMCW Systems

A. Transmitted and Received Signal Model

The PMCW radar system transmits continuous waves that are phase-modulated based on a PRBS. The transmitted signal consists of M pulses, where each pulse contains a code sequence of length N_c. The transmitted signal can be expressed as

$$s_{\text{TX}}(t) = \sum_{m=0}^{M-1} \sum_{n=0}^{N_c-1} c[n]\, e^{j2\pi f_c t}\, \Pi\left(\frac{t - mT - nT_c}{T_c}\right), \quad (1)$$

where $c[n] \in \{+1, -1\}$ and f_c denote the PRBS symbol of the n-th chip and the carrier frequency, respectively. In addition, T_c, $T(= N_c T_c)$, and $\Pi(\cdot)$ represent the chip duration, the pulse repetition interval (PRI), and the unit rectangular function, respectively.

When the transmitted signal is reflected from a point target located at range R with radial velocity v, the received signal undergoes a propagation delay and a Doppler frequency shift. The round-trip delay exhibits time-varying characteristics due to the relative motion between the radar and the target, which can be expressed as

$$\tau(t) = \frac{2R(t)}{c} = \frac{2(R_0 + vt)}{c} = \tau_0 + \frac{2v}{c}t, \quad (2)$$

where R_0, $\tau_0(= 2R_0/c)$, and c denote the initial range, the initial round-trip delay, and the speed of light, respectively. The Doppler frequency induced by the relative motion is given by

$$f_d = \frac{2v}{\lambda} = \frac{2vf_c}{c}. \quad (3)$$

Based on these parameters, the signal reflected from the target and arriving at the receiving antenna can be expressed as

$$s_{\text{RX}}(t) = \alpha s_{\text{TX}}(t - \tau(t)), \quad (4)$$

where α is a complex coefficient that accounts for path loss and target RCS. The received signal is down-converted to baseband by mixing with the local oscillator signal $e^{-j2\pi f_c t}$. The resulting intermediate frequency signal can be expressed as

$$\begin{aligned} s_{\text{IF}}(t) &= s_{\text{RX}}(t)\, e^{-j2\pi f_c t} \\ &= \alpha e^{-j2\pi f_c \tau(t)} \times \\ &\quad \sum_{m=0}^{M-1} \sum_{n=0}^{N_c-1} c[n]\, \Pi\left(\frac{t - \tau_0 - mT - nT_c}{T_c}\right). \end{aligned} \quad (5)$$

The phase term $-2\pi f_c \tau(t)$ can be expanded as

$$-2\pi f_c \tau(t) = -2\pi f_c \tau_0 - 2\pi f_c \frac{2v}{c} t = \phi_0 + 2\pi f_d t, \quad (6)$$

where $\phi_0 = -2\pi f_c \tau_0$ denotes the initial phase due to the target range. After applying a low-pass filter, the baseband signal becomes

$$s_{\text{BB}}(t) = \alpha e^{j\phi_0} e^{j2\pi f_d t} \sum_{m=0}^{M-1} \sum_{n=0}^{N_c-1} c[\text{mod}(n - d,\, N_c)]\,. \quad (7)$$

where $d(= \lfloor \tau_0 / T_c \rfloor)$ and $\text{mod}(\cdot)$ denote the delay index in chip units and the modulo N_c operation, respectively.

The baseband signal is then sampled with sampling period $T_s = T_c$. At the sampling instant $t = mT + nT_c$, the discrete-time signal can be expressed as

$$s[n, m] = \alpha e^{j\phi_0} c[\text{mod}(n - d,\, N_c)]\, e^{j2\pi f_d n T_c}\, e^{j2\pi f_d m T}. \quad (8)$$

where n $(n = 0, 1, \ldots, N_c - 1)$ and m $(m = 0, 1, \ldots, M - 1)$ denote the fast-time and slow-time indices, respectively. Here, the intra-pulse term $e^{j2\pi f_d n T_c}$ represents the phase rotation within a single pulse, which can degrade the code correlation performance. In contrast, the inter-pulse term $e^{j2\pi f_d m T}$ represents the phase change between pulses, which is used for velocity estimation.

B. 1-bit ADC

To reduce hardware complexity and power consumption, the full-resolution samples can be replaced by 1-bit quantization. Unlike conventional multi-bit ADC that preserve amplitude information, the 1-bit ADC retains only the sign of the signal by applying the signum function to both the real and imaginary parts. The quantized signal can be expressed as

$$s_{\text{1-bit}}[n, m] = \text{sgn}(\Re\{s[n, m]\}) + j\text{sgn}(\Im\{s[n, m]\}), \quad (9)$$

where the signum function is defined as

$$\text{sgn}(x) = \begin{cases} +1, & x > 0 \\ -1, & x \le 0 \end{cases}. \quad (10)$$

C. Range and Velocity Estimation

To extract range and velocity information, a two-stage processing is performed. First, range estimation is achieved by computing the circular correlation between the quantized

signal and the reference code sequence for each pulse. The correlation output can be expressed as

$$R[k,m] = \sum_{n=0}^{N_c-1} s_{\text{1-bit}}[n,m] c^*[\langle n-k \rangle_{N_c}], \tag{11}$$

where k $(k = 0, 1, \ldots, K-1)$ and $(\cdot)^*$ denote the range bin index and the complex conjugate, respectively. A correlation peak occurs at $k = d$, which corresponds to the target range.

Subsequently, velocity estimation is performed by applying the discrete Fourier transform (DFT) along the pulse axis. The DFT output is given by

$$X_{\text{1-bit}}[k,q] = \sum_{m=0}^{M-1} R[k,m]\, e^{-j\frac{2\pi mq}{M}}, \tag{12}$$

where q $(q = 0, 1, \ldots, Q-1)$ denotes the Doppler bin index. Here, K and Q represent the number of range and Doppler bins, respectively. The magnitude of RD map is defined as

$$S[k,q] = \left| X_{\text{1-bit}}[k,q] \right|, \tag{13}$$

and targets are detected by identifying peaks $S[k,q]$ that exceed a predefined threshold.

However, 1-bit quantization introduces nonlinear distortions such as elevated noise floor and sidelobe spreading in the RD map. A conventional approach to mitigate these artifacts is to apply a window function to the slow-time samples before the Doppler FFT [8]. The window function smooths the signal transition at the boundaries of the observation window, effectively suppressing spectral leakage caused by abrupt signal truncation. This windowing operation reduces the sidelobe levels in the Doppler spectrum at the cost of slight Doppler mainlobe broadening. In this paper, a three-term Blackman window is adopted as a baseline method due to its effective sidelobe suppression capability, which is defined as

$$w[m] = a_0 - a_1 \cos\left(\frac{2\pi m}{M-1}\right) + a_2 \cos\left(\frac{4\pi m}{M-1}\right), \tag{14}$$

where a_0, a_1, and a_2 are the standard Blackman window coefficients and m denotes the pulse index for $0 \le m < M$. By applying this window to the correlation output, the windowed DFT output can be expressed as

$$X_w[k,q] = \sum_{m=0}^{M-1} R[k,m]\, w[m]\, e^{-j\frac{2\pi mq}{M}}. \tag{15}$$

The windowing operation is a linear process that reshapes the spectral response by smoothing the abrupt edges of the observation interval. Therefore, it is effective in suppressing sidelobes caused by spectral leakage, which is also a linear phenomenon. However, 1-bit quantization inherently introduces nonlinear distortions, such as harmonic generation and intermodulation, which cannot be mitigated by linear operations. Therefore, we employ a learning-based approach to directly learn and suppress the nonlinear distortions caused by 1-bit quantization.

III. Proposed RD Map Reconstruction Method

A. Architecture of Proposed Neural Network

In 1-bit PMCW radar, sign-based quantization discards the true amplitude structure and relatively amplifies unwanted components such as leakage, sidelobes, and noise floor. Because amplitude information is irreversibly lost during quantization, the inherent autocorrelation properties of the PMCW sequence can no longer be preserved. As a result, the target structure in the RD response is attenuated, while distortion components emphasized by 1-bit quantization appear more prominently. Linear signal processing techniques such as windowing cannot restore amplitude information already lost during 1-bit quantization, which limits their ability to reconstruct the original RD response.

To overcome these limitations, we propose an end-to-end deep learning network that directly generates a refined and target-preserving RD map from a single 1-bit PMCW measurement. The proposed network follows an image translation framework based on the U-Net architecture and is trained to approximate the refined RD representation produced by an adaptive kurtosis-based filtering algorithm. This approach enables the network to learn nonlinear distortion patterns inherent to 1-bit quantization while preserving meaningful target responses.

The network adopts an encoder-decoder configuration consisting of three downsampling layers and three corresponding upsampling layers. The overall architecture of the proposed network is illustrated in Fig. 1. As the distorted 1-bit RD map passes through the encoder, the network progressively extracts hierarchical spatial features and suppresses background fluctuations. The bottleneck layer produces a compact latent representation that separates target components from distortion artifacts. The decoder then reconstructs a high-resolution RD map from this representation. To preserve spatial details that may be lost during downsampling, skip connections are employed between corresponding encoder and decoder layers. These connections maintain the continuity of mainlobe and sidelobe structures, prevent oversmoothing, and enable accurate peak reconstruction. The proposed network employs the rectified linear unit (ReLU) as the activation function. The network was trained with a batch size of 8, and early stopping was applied to prevent overfitting by terminating training after four consecutive epochs without improvement in validation loss.

B. Training Data Generation

To train the proposed network, 1,000 image pairs are generated. Each pair consists of a distorted 1-bit RD map and a corresponding cleaned RD map obtained by kurtosis-based filtering. To ensure robust generalization, the dataset covers various signal-to-noise ratio (SNR) levels, target scenarios, ranges, and velocities. The cleaned RD map is generated by applying a target-preserving refinement procedure to the complex-valued 1-bit RD map $X_{\text{1-bit}}$. This procedure suppresses non-ideal components using adaptive kurtosis-based

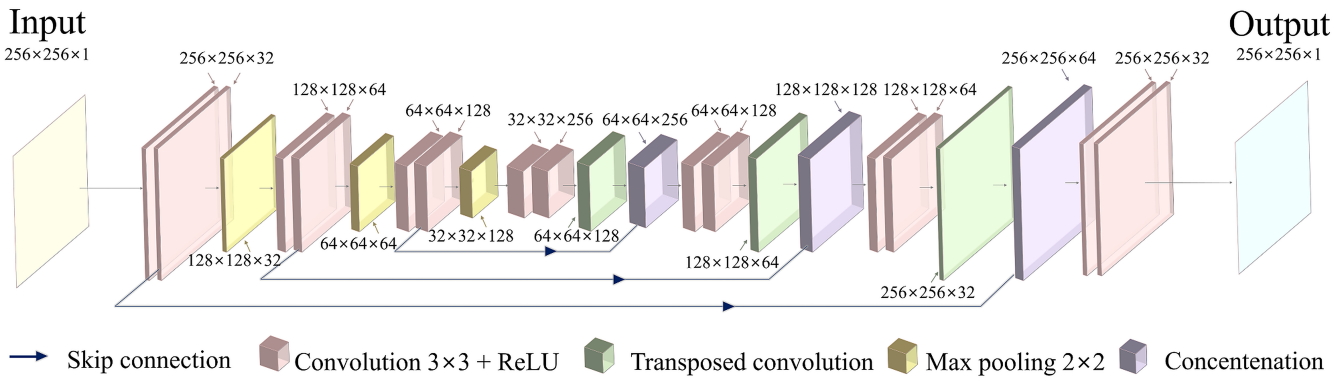

Fig. 1. Architecture of proposed neural network for RD map reconstruction.

detection. For each Doppler bin q, let $\mathbf{x}_q$ denote the magnitude along the range dimension of $X_{\text{1-bit}}$. A bin is identified as a target candidate if its sample kurtosis $\mathcal{K}(\mathbf{x}_q)$ exceeds an adaptive threshold and its peak magnitude surpasses the estimated noise floor η. To mitigate sidelobes, a power-based iterative suppression is applied, removing weaker candidates sharing the same range or Doppler bin as a dominant target.

The surviving target pixels form a mask $\mathcal{T}$, which is morphologically dilated to define a protection region. The protection region can be expressed as

$$\mathcal{P} = \mathcal{T} \oplus \mathcal{S}, \tag{16}$$

where $\oplus$ denotes the morphological dilation operator and $\mathcal{S}$ denotes a 6×4 rectangular structuring element. The cleaned RD map is then generated by clipping the magnitude of pixels outside $\mathcal{P}$ at the noise floor while leaving the phase unchanged. The magnitude of the cleaned RD map is given by

$$|X_{\text{clean}}| = U \odot |X_{\text{1-bit}}| + (1 - U) \odot \min(|X_{\text{1-bit}}|, \eta)\,, \tag{17}$$

where $\odot$ and U denote the Hadamard product and the binary protection mask derived from $\mathcal{P}$, respectively. The cleaned RD map X_{clean} serves as the ground-truth (GT), paired with the original distorted RD map $X_{\text{1-bit}}$ as the network input.

C. Loss Function

Let $F(\cdot)$ denote the proposed network. Given a distorted 1-bit RD map S as input, the network produces a reconstructed RD map $\hat{S} = F(S)$. The network is trained using a weighted combination of mean squared error (MSE) losses, which can be expressed as

$$\mathcal{L} = \frac{1}{2}\mathcal{L}_{\text{MSE}} + \frac{1}{2}\mathcal{L}_{\text{peak}}, \tag{18}$$

where $\mathcal{L}_{\text{MSE}}$ and $\mathcal{L}_{\text{peak}}$ denote the standard MSE loss and the peak-weighted MSE loss, respectively. The standard MSE loss is given by

$$\mathcal{L}_{\text{MSE}} = \frac{1}{KQ}\left\|\hat{S} - X_{\text{clean}}\right\|_F^2, \tag{19}$$

and the peak-weighted MSE loss is given by

$$\mathcal{L}_{\text{peak}} = \frac{1}{KQ}\left\|W \odot (\hat{S} - X_{\text{clean}})\right\|_F^2, \tag{20}$$

where $\|\cdot\|_F$ denote the Frobenius norm. In addition, W is a weighting matrix that assigns larger values to pixels exceeding a predefined threshold, and K and Q denote the dimensions of the RD map. This weighting scheme emphasizes accurate reconstruction of target peaks while maintaining overall background fidelity.

D. Inference Process

During inference, the input image is generated from the complex-valued RD map obtained through the 1-bit PMCW signal-processing chain. The complex RD map is first converted to magnitude and then transformed into the dB scale. The resulting values are clipped to a dynamic range of $[-50, 0]$ dB and normalized to $[0, 1]$ to form a single-channel 256×256 image. Since the RD map has a size of 255×256, zero-padding is applied to match the network input dimensions. This normalized image is fed into the trained network, which outputs a restored RD map in which quantization-induced distortions are suppressed while preserving the spatial structure of true targets.

IV. Performance Evaluation

A. Qualitative Evaluation

To evaluate the performance of the proposed method, we conducted simulations for a scenario with two targets located at ranges of 70 m and 30 m with velocities of 120 m/s and -100 m/s, respectively. The detailed specifications of the radar system used in the simulations are summarized in Table I.

Fig. 2 presents a qualitative comparison of RD maps obtained using different signal processing methods. Fig. 2 (a) shows the RD map generated by an adaptive kurtosis-based filtering algorithm. By exploiting the non-Gaussian statistical characteristics of target responses, this algorithm effectively isolates target components from background noise and distortions. Therefore, the resulting refined RD map is used as the GT reference for training and evaluation.

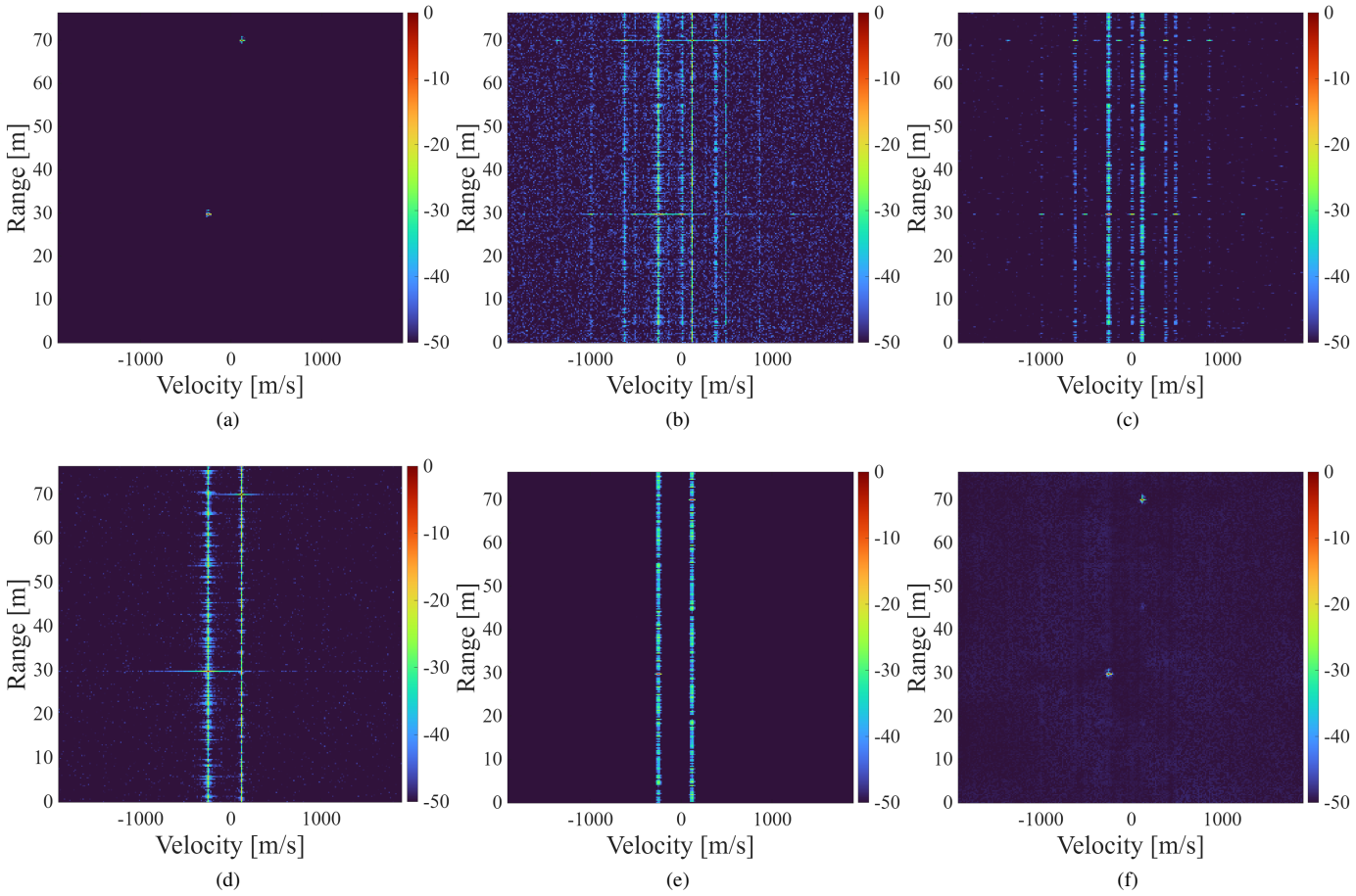

Fig. 2. RD maps for two targets at 10 dB SNR under different processing configurations: (a) GT generated by adaptive kurtosis-based cleaning, (b) 1-bit ADC with FFT, (c) 1-bit ADC with Blackman window, (d) multi-bit ADC with FFT, (e) multi-bit ADC with Blackman window, and (f) proposed method.

TABLE I
SPECIFICATIONS OF THE PMCW RADAR SYSTEM USED IN SIMULATIONS

Parameter	Value
Carrier frequency, f_c	77 GHz
Chip rate, R_c	0.5 GHz
Sequence length, $N_c = 2^m - 1$	255 ($m = 8$)
Number of pulses, M	256
PRI	510 ns
Range resolution, R_{res}	0.30 m

Fig. 2 (b) shows the RD map obtained directly from 1-bit ADC measurements using conventional FFT processing. As shown in the figure, the RD map exhibits a significantly elevated noise floor and sidelobe artifacts along both the range and Doppler axes. To mitigate these artifacts, a Blackman window is applied along the Doppler axis prior to the FFT, as shown in Fig. 2 (c). While the windowing operation partially reduces sidelobes in the Doppler domain, substantial sidelobes and background artifacts in the range domain still remain. This result highlights that windowing techniques are insufficient to address the nonlinear distortions introduced by 1-bit quantization.

For comparison, Figs. 2 (d) and (e) present the RD maps obtained using a conventional multi-bit ADC without and with Blackman windowing, respectively. Although multi-bit quantization preserves amplitude information and avoids the severe distortions observed in 1-bit systems, these results are still subject to inherent sidelobe levels determined by the autocorrelation properties of the PRBS and the spectral characteristics of the window function.

Finally, Fig. 2 (f) shows the RD map reconstructed by the proposed method. The proposed network successfully suppresses the noise floor and sidelobes in along both the range and Doppler dimensions, producing a result that closely resembles the GT shown in Fig. 2 (a). Overall, the qualitative results in Fig. 2 confirm that the proposed method overcomes the limitations of conventional linear processing methods and enables reliable RD map reconstruction in 1-bit PMCW radar systems, providing improved target visibility and resolution in both range and Doppler domains.

B. Quantitative Evaluation

To quantitatively assess the reconstruction performance, we employed four widely adopted metrics, namely peak sidelobe level (PSL), integrated sidelobe level (ISL), signal-to-interference-plus-noise ratio (SINR), and SINR gain [7].

The PSL measures the ratio between the strongest sidelobe and the mainlobe peak, which can be expressed as

$$\mathrm{PSL}_k(\mathbf{X}_{\text{1-bit}}) = 20\log_{10}\left(\max_{q\neq\hat{q}}(S[k,q])\right). \tag{21}$$

The ISL quantifies the total sidelobe energy relative to the mainlobe energy, which is given by

$$\mathrm{ISL}_k(\mathbf{X}_{\text{1-bit}}) = 20\log_{10}\left(\sum_{q=0,q\neq\hat{q}}^{M-1}(S[k,q])^2\right). \tag{22}$$

The SINR evaluates target detectability by measuring the ratio of the mainlobe peak power to the total power of sidelobes and background noise. Let P_{signal}, P_{sidelobe}, and P_{noise} denote the power of the target mainlobe, sidelobe components, and thermal noise, respectively. Then, the SINR can be expressed as

$$\mathrm{SINR} = 10\log_{10}\left(\frac{P_{\text{signal}}}{P_{\text{sidelobe}}+P_{\text{noise}}}\right). \tag{23}$$

Finally, the SINR gain quantifies the performance improvement relative to the multi-bit ADC with FFT, which is defined as

$$\Delta\mathrm{SINR} = \mathrm{SINR}_{\text{method}} - \mathrm{SINR}_{\text{ref}}, \tag{24}$$

where $\mathrm{SINR}_{\text{method}}$ and $\mathrm{SINR}_{\text{ref}}$ denote the SINR obtained using the corresponding processing method under evaluation and a multi-bit ADC with conventional FFT processing, respectively.

The quantitative performance metrics for each method are summarized in Table II. First, the results show that RD maps obtained using 1-bit ADC measurements suffer from severe performance degradation compared to the multi-bit ADC baseline. Specifically, both the 1-bit ADC with FFT and the 1-bit ADC with Blackman windowing exhibit an SINR loss of approximately 8.2 dB relative to the multi-bit ADC with FFT. This result indicates the inherent limitations of conventional linear processing techniques in mitigating the severe nonlinear distortions induced by 1-bit quantization. In contrast, the proposed method achieves substantial improvements across all evaluation metrics. Compared to the 1-bit ADC with FFT, the proposed method achieves a PSL of -46.19 dB and an ISL of -23.14 dB, corresponding to improvements of 31.5 dB in PSL and 15.96 dB in ISL, respectively. More notably, the proposed method outperforms even the multi-bit ADC with FFT, achieving an 18.35 dB improvement in PSL and a 4.94 dB gain in SINR. This demonstrates that the learning-based approach effectively suppresses nonlinear quantization artifacts beyond the capabilities of conventional signal processing methods, enabling reliable target detection in 1-bit PMCW radar systems.

TABLE II
PERFORMANCE COMPARISON OF RD MAP PROCESSING METHODS

Method	PSL (dB)	ISL (dB)	SINR (dB)	SINR gain (dB)
1-bit ADC with FFT	-14.69	-7.18	9.79	-8.26
1-bit ADC with Blackman	-12.15	-8.30	9.81	-8.24
Multi-bit ADC with FFT	-27.84	-22.41	18.05	0
Multi-bit ADC with Blackman	-26.49	-9.97	18.99	0.94
Proposed method	-46.19	-23.14	22.99	4.94

V. CONCLUSION

In this paper, we proposed a deep learning-based method to reconstruct high-quality RD maps for 1-bit quantized PMCW radar systems. While 1-bit quantization offers significant advantages in power efficiency and hardware simplicity, it introduces severe nonlinear distortions in the RD domain, which degrade target detection performance. To address this challenge, we developed a U-Net architecture trained using paired datasets consisting of distorted RD maps and corresponding refined RD maps. The refined RD maps were generated using an adaptive kurtosis filtering algorithm, which enabled supervised training without the need for manual annotation. Simulation results demonstrated that the proposed method effectively suppressed nonlinear distortions, outperforming not only conventional windowing-based processing for 1-bit ADCs but also multi-bit ADC-based processing. These results confirmed that the proposed method enabled reliable target detection in 1-bit PMCW radar systems while maintaining their inherent advantages in power efficiency and cost effectiveness.

ACKNOWLEDGMENT

This work was supported by the National Research Foundation of Korea (NRF) grant funded by the Korea government (MSIT) (No. RS-2024-00405510).

REFERENCES

[1] W. Zhou, R. Zhang, G. Chen, and W. Wu, "Integrated sensing and communication waveform design: A survey," *IEEE Open Journal of the Communications Society*, vol. 3, pp. 1930–1949, Oct. 2022.

[2] H. Ma, "Integrated sensing and communication - The ISAC technology," *2024 IEEE 2nd International Conference on Sensors, Electronics and Computer Engineering (ICSECE)*, Jinzhou, China, Aug. 2024, pp. 225–229.

[3] A. Bourdoux *et al.*, "PMCW waveform and MIMO technique for a 79 GHz CMOS automotive radar," *2016 IEEE Radar Conference (RadarConf)*, Philadelphia, PA, USA, May 2016, pp. 1–5.

[4] C. Park, J.-H. Park, T. Jeong, J. Joung, and S. Lee, "Efficient frame structure design of PMCW radar based on Golay sequence in 802.11ad preamble," *IEEE Internet of Things Journal*, vol. 12, no. 24, pp. 53177–53188, Dec. 2025.

[5] F. Foroozmehr, M. Modarres-Hashemi, and M. M. Naghsh, "One-bit PMCW radar: Designing binary transmit code and receive filter via a worst-case approach," *IEEE Transactions on Vehicular Technology*, vol. 73, no. 12, pp. 19774–19779, Dec. 2024.

[6] M. Bauduin and A. Bourdoux, "Impact of phase noise on FMCW and PMCW radars," *2023 IEEE Radar Conference (RadarConf23)*, San Antonio, TX, USA, May 2023, pp. 1–6.

[7] Y. Wang, J. Li, and P. Stoica, "GAN-based range-Doppler map restoration for one-bit PMCW automotive radar," *IEEE Transactions on Vehicular Technology*, vol. 72, no. 8, pp. 9876–9889, Aug. 2023.

[8] X. Shang, H. Zhu, and J. Li, "Range-Doppler imaging via one-bit PMCW radar," *2020 IEEE International Conference on Acoustics, Speech and Signal Processing (ICASSP)*, Barcelona, Spain, May 2020, pp. 4702–4706.